vanadium oxide (V_2O_5) thin film placed inside the gas cell. V_2O_5 thin film has been used in electrochromic coloration, but little is known regarding if, and how, the atomic/electronic structures of a V_2O_5 thin film were modulated at the same time.

Figure 2(a) illustrates the L-edge spectra taken from gasochromic V_2O_5 under color switching. Two more spectra recorded from VO_2 and V_2O_5 crystals were added in to serve as references. A typical V L-edge spectrum has two broad peaks centered at about 518 and 525 eV that feature the transitions from two spin-orbit split 2*p* states to 3*d* states. Considering the 2*p* orbital is localized on V, the L-edge intensity is directly proportional to the unoccupied *d*-character. As shown in **Fig. 1(a)**, the main peak of the V L_3-edge shifts to a lower energy as the reaction proceeds (marked by arrows). This is an indication of vanadium receiving charge upon hydrogen absorption.

In addition to the change of absorption resonance energy, the profile of a XAS spectrum is informative too. As shown in **Fig. 2(b)**, V L_3 peak is decomposed into four components that each of them corresponds to a specific V 3*d* orbital symmetry (A: $3d_{xz}$ & $3d_{yz}$, B: $3d_{xy}$, C: $3d_{x^2-y^2}$ and D: $3d_{z^2}$). A fit of these spectra recorded at three coloration stages (10, 30 and 60 min) returns with the findings that the coloration leads to different intensity variation among the four sub-components of L_3-edge. In particular, with the increase of intensity at component A (more empty *d* states, weaker hybridization along *z*-axis) and decrease of intensity at component B (less empty *d* states, stronger hybridization at basal plane), it is apparent that coloration leads to a strengthened interaction between V atoms and basal oxygen. This finding is consistent with the intensity variation found between components C and D that count the electron density distributed along all three axes (*x,y,z*). According to **Fig. 2(c)**, the increase of intensity ratio between $d_{x^2-y^2}$ and d_{z^2} is a consequence of the central V atom moving closer to the basal plane after the gasochromic coloration.

In summary, Dong used operando XAS measurements to reveal that, for a V_2O_5 film going through the gasochromic coloration process, there are not only changes on the charge state of vanadium, but also modification on the local atomic symmetry of V_2O_5. The injected hydrogen atoms cause a structural deformation from pyramid-like to octahedral-like symmetry. (Reported by Der-Hsin Wei)

This report features the work of Chung-Li Dong and his collaborators published in Phys. Chem. Chem. Phys. ***19****, 14224 (2017).*

TLS 20A1 BM – (H-SGM) XAS

- XANES, XFS, PSD, XPS, AES
- Materials Science, Chemistry, Surface, Interface and Thin-film Chemistry, Condensed Matter Physics

References

1. L. Long, and H. Ye, Sci. Rep. **4**, 6427 (2014).
2. Y.-R. Lu, T.-Z Wu, H.-W. Chang, J.-L. Chen, C.-L. Chen, D.-H. Wei, J.-M. Chen, W.-C. Chou, and C.-L. Dong, Phys. Chem. Chem. Phys. **19**, 14224 (2017).

Novel Route to Effective Doping at Heterostructure Interfaces

Doping carriers across interfaces of thin film heterostructures is an extremely sensitive and important requirement for controlling their emergent properties. Atomically precise termination is now shown to be a novel route to effectively dope superconductor/ferromagnet ($YBa_2Cu_3O_{7-x}/La_{0.7}Ca_{0.3}MnO_3$) heterostructures.

Heterostructures hold tremendous potential for creating emergent properties not seen in single phase bulk materials. Since the discovery of a 2-D (2-dimensional) electron gas at the $LaAlO_3$-$SrTiO_3$ interface,[1,2] there have been several important results revealing unexpected properties of interfaces: controlling a 2D electron gas with a ferroelectric,[3] orbital reconstruction at superconductor-ferromagnet interfaces,[4] *etc*.

In this article, we discuss the work carried out by Ying-Hao Chu (National Chiao Tung University) and his co-workers,[5] which reported on the successful development and observation of termination control for effectively dop-

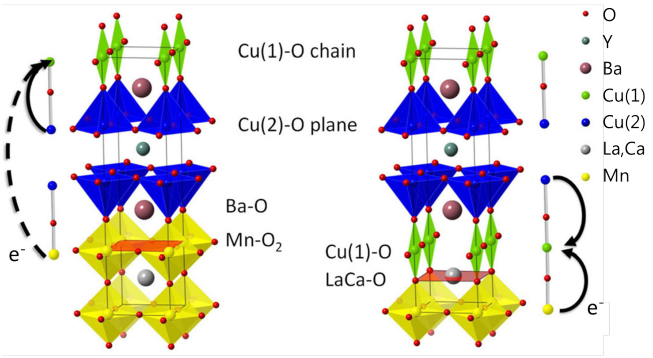

(a) MnO_2 -terminated (b) $La_{0.7}Ca_{0.3}O$ -terminated

Fig. 1: Epitaxial design of heterointerfaces: schematic of the interfacial control of LCMO/YBCOd with different interfaces. (a) Shows the MnO_2-terminated interface ($La_{0.7}Ca_{0.3}O$-MnO_2-BaO-CuO_2), for which the charges are very difficult to transfer because CuO chains are very far from the interface (indicated by a dashed line) while (b) shows the $La_{0.7}Ca_{0.3}O$-terminated (MnO_2-$La_{0.7}Ca_{0.3}O$-CuO_2-BaO) interface which uses an SRO layer, and for which electrons can transfer easily from LCMO to YBCO due to the CuO chains at the interface (indicated by solid lines). [Reproduced from Ref. 5]

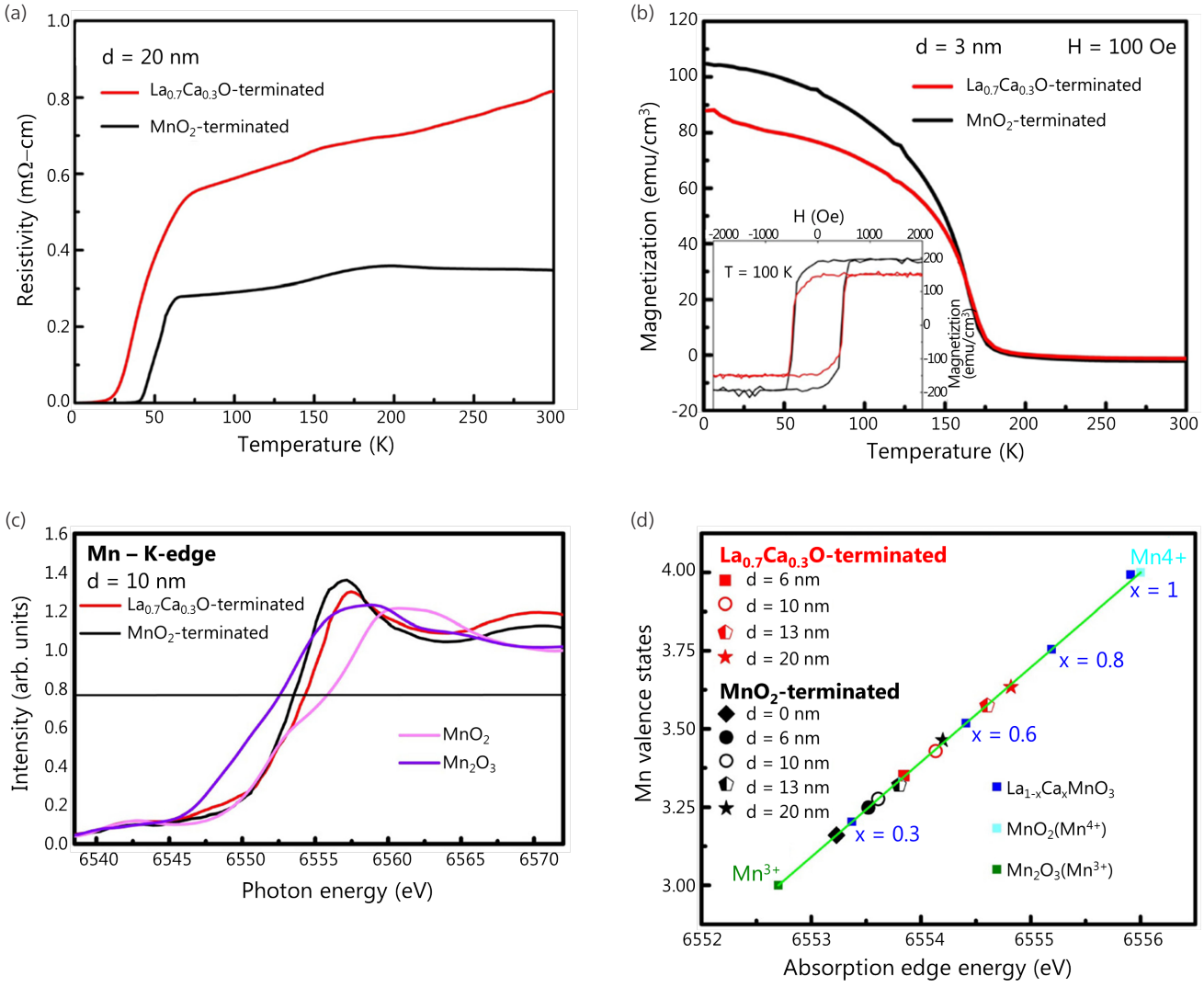

Fig. 2: (a) Transport properties of LCMO/YBCOd with different interfaces: YBCO thickness dependence of the superconducting transition temperature with either MnO_2- or $La_{0.7}Ca_{0.3}O$-terminated interfaces. (b) Low-temperature magnetization as a function of the YBCO layer thickness for two different interfaces. (c) The Mn valence state vs. the absorption edge energy of the MnO_2-terminated (black symbols) and $La_{0.7}Ca_{0.3}O$-terminated (red symbols) samples. $La_{1-x}Ca_xMnO_3$ (where x = 0, 0.3, 0.6, and 1) was used as the reference samples, combined with the Mn_2O_3 (Mn^{3+}) and MnO_2 (Mn^{4+}) standard samples to determine the Mn valence state. (d) The Mn valence state as a function of YBCO thickness for the two different interfaces. [Reproduced from Ref. 5]

ing a superconductor-ferromagnet heterostructure of $YBa_2Cu_3O_{7-x}/La_{0.7}Ca_{0.3}MnO_3$ (YBCO/LCMO). The authors achieved an atomically precise interface control of YBCO/LCMO heterostructures, that is, they succeeded to make heterostructures with a MnO_2-terminated (**Fig. 1(a)**) interface and a $La_{0.7}Ca_{0.3}O$-terminated **(Fig. 1(b)**) interface. The MnO_2-terminated heterostructure corresponds to the STO($SrTiO_3$)/$LCMO_{10}$ nm/YBCOd structure while the $La_{0.7}Ca_{0.3}O$-terminated one corresponds to the STO/$SRO_{2.5u.c.}$ ($SrRuO_3$)/$LCMO_{10\,nm}$/YBCOd structure. The authors first used high-angle annular dark-field scanning transmission electron microscopy to confirm the two distinct terminations and interfaces. The authors then fixed the LCMO layer thickness to 25 units cells (~10 nm) and varied the thickness d of the YBCO layer. From a systematic set of electrical resistivity and magnetization measurements, they could establish that the MnO_2-terminated samples showed a consistently higher superconducting transition temperature T_C (**Fig. 2(a)**) and a larger magnetization (**Fig. 2(b)**). For the lowest thickness of d = 6 nm, an intriguing result was obtained: the $La_{0.7}Ca_{0.3}O$-terminated sample was insulating while the MnO_2-terminated sample was superconducting with an onset T_C ~40 K.

Subsequently, synchrotron based X-ray absorption spectroscopy (XAS) and X-ray magnetic circular dichroism (XMCD) studies were carried out at NSRRC to understand the changes in the electronic structure. From a systematic study of the Mn K-edge and L-edge XAS, they could show that the Mn valence depends on the termination and changes systematically with the thickness d (**Fig. 2(c)**). In addition, the suppression of the magnetization in the $La_{0.7}Ca_{0.3}O$-terminated samples by magnetization and XMCD measurements was consistently confirmed. Thus, the authors could show that the MnO_2-terminated samples always showed (i) a larger magnetic moment of Mn, (ii) a lower valence state of Mn, and (iii) a higher superconducting T_C compared to the $La_{0.7}Ca_{0.3}O$-terminated samples (**Fig. 2(d)**).

Since the results clearly indicated a relationship between larger FM fluctuations with stronger superconductivity, it could be concluded that the conventional scenario of ferromagnetism competing superconductivity does not hold for these heterostructures. And since it is known from earlier work that electronic charge gets transferred from Mn to Cu ions across the interface and induces a major reconstruction of the orbital occupation and orbital symmetry in the interfacial CuO_2 layers,[3] the authors have proposed that the differences in the interfacial structure (**Fig. 1**) of the MnO_2-terminated and $La_{0.7}Ca_{0.3}O$-terminated interfaces leads to a difference in charge-transfer for the two cases. This is fully consistent with the lower Mn-valency of the MnO_2-terminated interfaces and leads to their higher superconducting T_C values. The results thus conclusively show that termination control is a useful degree of freedom to effectively manipulate the doping and physical properties of heterostructures. (Reported by Ashish Chainani)

This report features the work of Ying-Hao Chu and his co-workers published in App. Phys. Lett. ***110****, 032402 (2017).*

TLS 11A1 BM – (Dragon) MCD, XAS
TLS 20A1 BM – (H-SGM) XAS

- MCD, XAS
- Condensed Matter Physics, Materials Science

References

1. A. Ohtomo and H. Y. Hwang, Nature **427**, 423 (2004).
2. J. Biscaras, N. Bergeal, A. Kushwaha, T. Wolf, A. Rastogi, R. C. Budhani, and J. Lesueur, Nat. Commun. **1**, 89 (2010).
3. V. T. Tra, J. W. Chen, P. C. Huang, B. C. Huang, Y. Cao, C. H. Yeh, H. J. Liu, E. A. Eliseev, A. N. Morozovska, J.-Y. Lin, Y. C. Chen, M. W. Chu, P. W. Chiu, Y. P. Chiu, L. Q. Chen, C. L. Wu, and Y.-H. Chu, Adv. Mater. **25**, 3357 (2013).
4. J. Chakhalian, J. W. Freeland, G. Cristiani, H.-U. Habermeier, G. Khaliullin, M. Van Veenendaal, and B. Keimer, Science **318**, 1114 (2007).
5. V. T. Tra, R. Huang, X. Gao, Y.-J. Chen, Y. T. Liu, W. C. Kuo, Y. Y. Chin, H. J. Lin, J. M. Chen, J. M. Lee, J. F. Lee, P. S. Shi, M. G. Jiang, C. G. Duan, J. Y. Juang, C. T. Chen, H. T. Jeng, Q. He, Y.-D. Chuang, J.-Y. Lin, and Y.-H. Chu, App. Phys. Lett. **110**, 032402 (2017).